

Chemical Exchange Saturation Transfer effect from Phospho-creatine (PCr) and Adenosine-tri-phosphate (ATP)

M. Haris¹, K. Cai¹, A. Singh¹, V. B. KC¹, H. Hariharan¹, and R. Reddy¹
¹CMROI, Radiology, University of Pennsylvania, Philadelphia, Pennsylvania, United States

Background

Phospho-creatine (PCr) and Adenosine tri-phosphate (ATP) are the major energy sources/reservoirs in the biological system. The concentration of ATP and PCr is varied in the different organs. The ATP concentration in brain, heart and muscle is ~3-4mM, ~6mM and ~10mM, respectively. On the other hand PCr which is a major source of energy reservoir present around 5-6mM in brain, 10mM in heart and around 33.5mM in muscles. Alterations of these energy-rich compounds have been reported in various disease conditions including tumors, heart infarction and muscular disorders. ³¹P MRS has been widely used to detect the signal from these metabolites. Phosphorous imaging of PCr has been previously reported utilizing MT effects between Pi and PCr. Chemical Exchange Saturation Transfer (CEST) technique has been previously used to exploit the chemical exchange between the labile amide proton (-NH) and bulk water to map pH changes in tissues as well as the protein content in the brain, while -OH exchange was used to measure the proteoglycan concentration in cartilage as well as glycogen concentration changes in the liver¹⁻⁴. Here, for the first time we report the CEST effect from PCr and ATP in-vitro on phantoms by exploiting their labile amine protons (-NH₂) as well as a PCr MRI CEST map from resting calf muscle.

Materials and Methods

MRS Spectroscopy: All the spectroscopic experiments were performed on 9.4 T vertical bore scanner (Inova; Varian, Palo Alto, CA) in 5 mm NMR tubes using 5 mm radiofrequency (RF) probe at room temperature. All the experiments were performed at room temperature. **¹H NMR Spectroscopy of Exchangeable Proton:** To explore the presence of exchangeable protons in ATP and PCr (Sigma Aldrich, USA), 100mM PCr and 50mM ATP solutions were prepared. **¹H-spectroscopy** was performed by gradual addition of D₂O (0%, 50% and 99.8%) using TR=3s, Te=4ms, number of averages = 64). **CEST Z-spectrum Acquisition:** Z-spectra from all samples were acquired over ±5ppm relative to the bulk water resonance frequency in steps of 0.125ppm with a 1 second pre-saturation square pulse at 127Hz B₁. The repetition time was 4 seconds. The integrated area under the bulk water peaks were calculated and plotted against the pre-saturation frequencies to generate the Z-spectra. **Exchange Rate Measurement:** exchange rate both from PCr and ATP were calculated using the method described in detail elsewhere⁵. **Phantom Imaging at 7T and 3T MRI:** Different concentrations of PCr (5, 10, 15, 20, 33 and 50mM, pH=7.0) and ATP solutions (5, 10, 15, 20mM, pH=7.0) were prepared in small glass tubes (1.5 cm diameter) and immersed in a beaker containing PBS. The CEST imaging was performed on 7T and 3T Siemens whole-body clinical scanner (Siemens Medical Solutions, Malvern, PA). CEST images were acquired at peak B1 of 150 Hz and 10 second saturation duration, with a flash readout, using a Hanning windowed saturation pulse train of 100 pulses. The sequence parameters were: slice thickness = 5mm, GRE flip angle=10°, GRE readout TR=5.6ms, TE =2.7 ms, field of view =120*120 mm, matrix size =192*192, and one saturation pulse and 64 acquired segments at every 15s. For the same parameters CEST imaging from PCr solutions were also obtained on 3T at 50% duty cycle. We also obtained CEST images from a normal human volunteer calf muscle at 7T. The human studies were performed under an Institutional IRB approved protocol. CEST contrast was calculated at ±2.5ppm for PCr and ±2ppm for ATP by normalizing with 20ppm signal using the equation:- CEST=100*(S_{ve}-S_{ve})/S₀, where S₀ is the acquired MR signals at 20ppm for phantoms and CEST = 100*(S_{ve}-S_{ve})/S_{ve} for the human study to minimize direct saturation and MT effects. B1 and B0 maps were also acquired and used to correct the MI CEST contrast as described previously⁵.

Results and Discussion

The spectra in presence of D₂O clearly depict the presence of exchangeable protons both in PCr and ATP (Fig. 1&2). In PCr the exchangeable -NH₂ protons were present at two frequency offset downfield to bulk water proton resonance i.e. ~1.8ppm and ~2.5ppm. Labile proton at ~1.8ppm was from creatine (Cr) and at ~2.5ppm was from PCr. The presence of Cr is due to the conversion of PCr into Cr. In ATP, the labile -NH₂ protons were detected at ~2ppm downfield to the bulk water proton resonance. The Z-spectra from PCr and ATP phantoms show the clear CEST peak at ~2ppm and ~2.5ppm respectively (Fig. 1&2). The measured exchange rates were ~180 s⁻¹ in PCr and ~150s⁻¹ in ATP. On comparing to the chemical shift difference both at 7T (Δω (PCr)=4.7x10³ rad/s and Δω (ATP)=3.7x10³ rad/s) and 3T (Δω (PCr)=2x10³ rad/s and Δω (ATP)=1.6x10³ rad/s) the exchange rate of both PCr and ATP -NH₂ protons are in regime of slow exchange rate and satisfy the condition (Δω>k) required for the CEST effect. Both PCr and ATP phantoms show the linear relationship with concentration (Fig 3&4). The PCr CEST contrast at 3T was less than 7T. This can be attributed to the reduced duty cycle of the saturation pulse. The preliminary human CEST images also seem encouraging. We are in process of implementing the current technique to investigate mapping of PCr and Cr in-vivo on human calf muscles both at 3T and 7T and monitor exercise related changes in these metabolites.

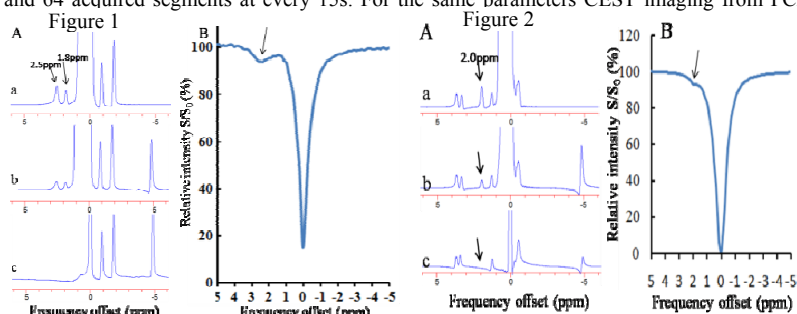


Figure 1&2: NMR spectra from 100mM PCr and 50mM ATP solutions. PCr shows the two peaks at 1.8 and 2.5ppm (Fig 1. A, a) while ATP shows one peak at 2ppm downfield to the bulk water (Fig 2. A, a). After addition of 50% D₂O the amplitude of all the peaks decrease (b) and completely disappear after addition of 99.9% D₂O (c), indicating that these resonances are exchangeable groups. In PCr peak present at the 1.8ppm is from creatine -NH₂, while the other peak at 2.5ppm is from PCr -NH₂. Z-spectra from PCr shows CEST effect at 2.5ppm (Fig 1, B, arrow), while ATP shows CEST effect at 2ppm downfield to the bulk water resonance (Fig 2, B, arrow).

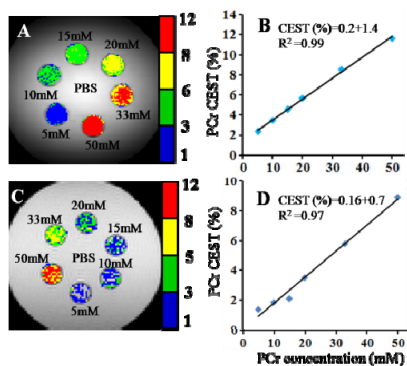


Figure 3: MRI CEST images both at 7T and 3T. PCr CEST contrast overlay on the CEST image obtained at -2.5ppm (A&C). Figure B & D reflects the linear dependence of CEST contrast on PCr concentration. At 7T CEST effect is higher than at 3T.

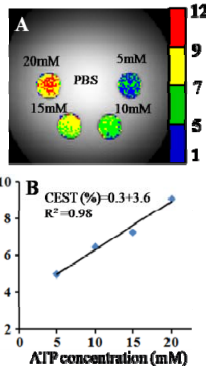


Figure 4: The ATP CEST contrast overlay on the CEST image obtained at -2.0ppm (A). Figure B reflects the linear dependence of ATP CEST contrast on ATP concentration.

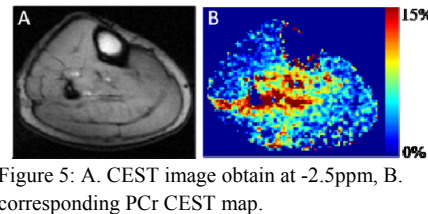


Figure 5: A. CEST image obtained at -2.5ppm. B. corresponding PCr CEST map.

References:

1. Zhou et al. Nat Med. 2003;9:1085-90. 2. Jones et al. Magn Reson Med. 2006;56:585-92. 3. Zijl PC et al. PNAS USA 2007;104:4359-64. 4. Ling et al. PNAS USA 2008;105:2266-70. 5. Haris et al. Neuroimage. 2010.

Acknowledgement: This work was performed at NIAMS and NCRR supported Biomedical Technology and Research center